JOURNAL OF MATERIALS SCIENCE: MATERIALS IN MEDICINE 7 (1996) 657–663

TiNi shape memory clamps with optimized structure parameters

P. FILIP, J. MUSIALEK*, H. LORETHOVÁ, J. NIESLANIK*, K. MAZANEC
TU of Ostrava, Institute of Materials Engineering, tř 17.listopadu 708 33 Ostrava-Poruba, Czech Republic
** Municipal Hospital Ostrava Fifejdy, Orthopaedic clinic, Nemocniční 20, 728 80 Ostrava, Czech Republic*

The different treatments of TiNi shape memory alloys applied as a material for so-called TiNi clamps and their influence on substructure parameters and deformation behaviour are discussed. The forces generated in fine-grained materials with higher dislocation density are stable after the cooling of the clamp to body temperature, which is a necessary condition for stable fixation of bone fragments. The forces generated and reversible strains depend on the substructure state and system stiffness parameter. The "yield point" and the "elastic moduli" are modified by controling the B2/B19′ interface mobility. The mechanical parameters obtained after annealing at 400 and 500 °C, respectively, following the 15% cold-working reduction are optimal for the TiNi clamp design. The TiNi clamps with optimal properties have been used in a total of 68 patients. The new TiNi clamps enhance the fixation of the bone fragments involved, helping to prevent redislocation and provide the ability for earlier active rehabilitation.

1. Introduction

The near-equiatomic titanium-nickel intermetallics belong to a class of "memory" materials that exhibit shape memory behaviour. Components and devices made of memory materials can remember their original shape after significant deformation and shape recovery occurs either immediately after the unloading of the deformed part (pseudoelasticity, PE) or after its subsequent heating above a critical temperature (shape memory effect, SME) [1–4].

The shape memory effect is related to a martensitic phase transformation, and the memory strain (the recoverable strain) is brought about by a stress-induced martensitic phase transformation or by reorientation of the martensite variants during stressing. During unloading (PE) or after heating (SME), the most favourably oriented martensite B19′, with respect to the stress applied, transforms back to the high temperature phase B2 and shape recovery occurs. The fundamental memory parameters and the mechanical behaviour of memory alloys are dependent on the conditions at which the martensitic phase transformation, the reorientation of martensitic variants, as well as the reversible phase transformation, occur. There is much information concerning deformation behaviour of annealed polycrystalline TiNi alloys and single crystals [4] and many applications are limited to the use of annealed alloys. In some of our previous papers, we have described the influence of work hardening and subsequent heat treatment on the substructure and final mechanical properties of TiNi shape memory alloys [5–10]. These results were more or less confirmed in other works [11] and it is clear, that the optimal treatment of memory alloys can lead to a better and more efficient use of memory material.

The intermetallic compound TiNi has an excellent resistance to corrosion and several researchers have found that TiNi displays biocompatibility [12–14] so a great number of medical applications, from external devices to temporary and permanent implants, have been used and suggested [15–19].

This paper concentrates on the structure optimization of newly designed and developed TiNi shape memory clamps. The new clamps differ from those developed previously [15, 18, 19] partially by design, but the most important difference lies in the structural parameters leading to optimized stiffness, strain recovery and generated forces accompanying the shape memory effect.

The aim of structure optimization is to make a material (TiNi clamps) which will guarantee:

- optimal transformation temperatures with respect to body temperature;
- the production of physiological forces when shape memory effect occurs and the bone fractions are compressed during heating;
- constant level of fixation forces after heating, and following cooling of the clamp to body temperature;
- the possibility to predeform and eventually further adjust the TiNi clamps at room temperature (without the necessary cooling) if a further modification of the shape is required during the operation.

0957–4530

TABLE I Transformation temperatures of TiNi materials after different treatment

		Treatment regime			
	15%	400 °C/1 h/w[a]	500 °C/1 h/w	600 °C/1 h/w	900 °C/1 h/w
M_s [°C]	−2	0	4	5	5
M_f [°C]	−26	−12	−16	−14	−14
A_s [°C]	16	16	17	16	16
A_f [°C]	43	41	36	35	35

[a] w – quenching in water.

2. Experimental procedures

The vacuum induction melting technique was used to prepare the binary 49.9 at% Ti–50.1 at% Ni alloys. As-cast TiNi alloy ingots, weighing approximately 10 kg, were homogenized, extruded into rods 12 mm in diameter, hot-forged and cold-drawn into wires with a diameter of 2.5 mm. The wires were annealed at 800 °C in an argon atmosphere after every 30% reduction. The last cold reduction was 15% and the wires were annealed in an argon protective atmosphere at 400, 500, 600 and 900 °C, respectively, for 1 h while shaping the clamps. Transformation temperatures were estimated from resistance versus temperature dependence and are given in Table I.

Tensile tests were carried out by using an Instron 1196 tensile test machine with specific grips enabling it to deform the clamps at room temperature. The clamps were deformed at a strain rate $\varepsilon = 0.012\ s^{-1}$ to the maximum recoverable strain ε_{rm} (completely reversible after appropriate heating). After predeformation the clamps were unloaded and subsequently heated to temperatures between 45 and 80 °C using warm water. The different testing configurations were used to reach a specific stiffness parameter (SP) of the system during the shape memory effect. The forces generated (F_g) during heating of the predeformed specimens were measured.

The substructure of the TiNi clamps was studied using a transmission electron microscope Jeol 200 CX (TEM). Thin foils for TEM were prepared from wires with 2.5 mm diameter. The spark-cut foils were mechanically ground and subsequently polished in a solution of CH_3COOH and $HCLO_4$ using a Tenupol twin-jet polisher ($T = 5$ °C and U = 15 V).

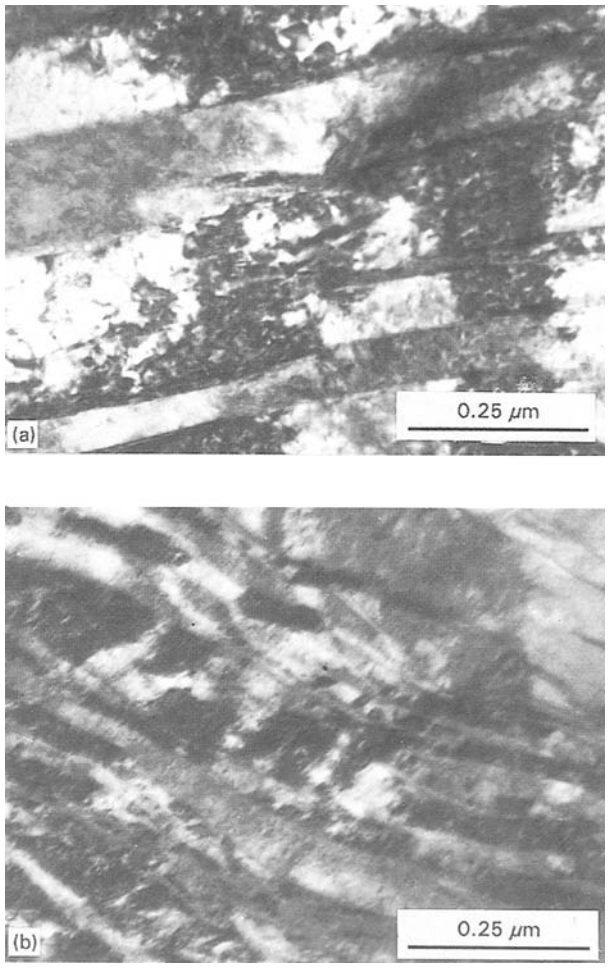

Figure 1 Structure of work-hardened alloy (reduction 15%) consisting mostly of B2 high-temperature phase (a) and small amounts of stabilized martensite B19′ (b).

3. Results and discussion

3.1. Influence of work hardening and annealing on the structure of TiNi

During cold-drawing, the transformation plasticity of the TiNi material is exhausted and work hardening occurs [4, 6, 9]. The structure of the work hardened alloy is formed mostly of high-temperature phase B2 (Fig. 1a) and only small amounts of stabilized martensite B19′ were detected after final cold-drawing with 15% reduction (Fig. 1b). Elongated grains of the B2 high-temperature phase and enhanced dislocation density (Fig. 1a) are typical of cold-drawn wires. The wavy bands of B19′ martensite plates (Fig. 1b) indicate that serious plastic deformation of the matrix occurs during drawing. The generated dislocations stabilize the B2 phase (the M_s temperature is the lowest one in this case, see Table I) which corresponds with previously described results [4, 6, 11]. It has been found that internally slipped martensite forms in cold-worked alloys [20] and the reversible transformation requires more energy when compared with typically observed internally twinned martensite. The B2/B19′ interfaces are blocked by dislocations and martensite plates cannot easily shrink [4, 6, 8]. For this reason, the A_f temperature is highest in work-hardened specimens even if the internal elastic stresses contribute to the back transformation B19′ → B2, as has been theoretically as well as experimentally evidenced in other works [21, 22]. The "duplex"substructure consisting of B2 phase and B19′ retained

martensite is stable up to recrystallization temperatures (500 °C). The R-phase formation was not found in the alloys investigated which contrasts with the results obtained for hot-rolled TiNi alloys with similar composition [6].

Annealing at 400 °C leads to a decrease of dislocation density, but stabilized martensite was still observed in the structure. The lower dislocation density (as a consequence of matrix restoration) results in the observed changes of the transformation temperatures (Table I). The substructure of the specimen annealed at 500 °C is presented in Fig. 2. It is evident that the recrystallization process started at 500 °C and the fine-grained B2 structure is obtained after annealing at this temperature. After annealing at 600 °C, equiaxed B2 grains are observed, and annealing at 900 °C led to further growth of B2 grains and decrease of dislocation density (Fig. 3).

The substructure of the materials predeformed to a maximum reversible strain ε_{rm} is completely martensitic (Fig. 4). As follows from Fig. 4, the stress-induced martensite (SIM) transformations occur during loading, and the preferrentially oriented martensitic plates are typical of predeformed specimens.

3.2. Deformation behaviour

3.2.1. Stress–strain dependences

The stress–strain curves of TiNi alloys are strongly dependent on the content of the three following fundamental phases: the high-temperature B2 phase, the R-phase and the B19′ martensite [1, 4]. As already mentioned, the alloy types investigated do not contain the R-phase and a dominant presence of austenite is typical at room temperature. The stress–strain dependences of the alloys investigated after different annealing conditions are presented in Fig. 5. Curve 1 represents the work-hardened state and curves 2, 3, 4 and 5, respectively, represent the tensile behaviour of materials annealed at 400, 500, 600 and 900 °C, respectively.

At the critical stress σ_{Mi}, the typical easy deformation with $d\sigma/d\varepsilon \rightarrow 0$ occurs. The strain reached before the value σ_{Mi} is usually regarded as an elastic strain. Similarly, it is considered that after the transformation and/or reorientation capacity is exhausted, the plateau is followed by elastic straining of the martensite. Both the observed slopes in the stress–strain curves are often held as quantities representing "elastic moduli". This is not absolutely true, because the "elastic moduli" are strongly dependent on the work-hardening stage. Owing to the higher dislocation density, the "plateau" is steeper in work-hardened alloys when compared with the deformation behaviour of annealed specimens. The interface mobility is lowered as a consequence of interface interaction with dislocations present in the matrix. Comparing the annealed specimens with the work-hardened state, the apparent decrease of "elastic moduli" at the start of straining and the increase at strains greater than those at which an outstanding plateau occurs, are typical. The specimens annealed at 500 °C differ from those annealed at 900 °C, with the former having a higher dislocation density and finer grain size. The stress-induced transformation occurs, to some smaller extent, at low strains as well as in the region following the easy deformation range, and modification of this effect causes the changes in "elastic moduli". This means that the dislocations present in the matrix are effective obstacles for martensite growth during SIM formation and the "elastic moduli" are higher in materials

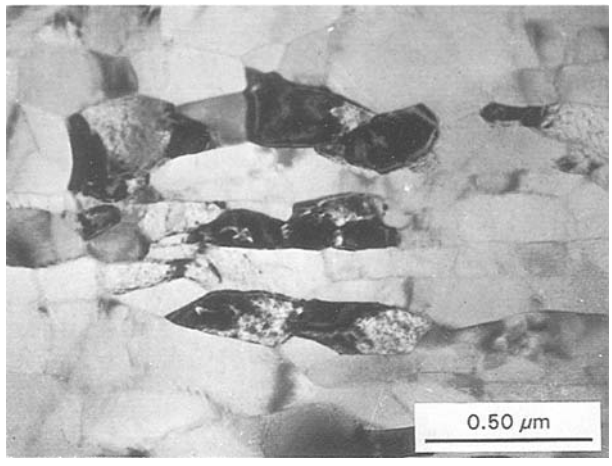

Figure 2 Structure of alloy annealed at 500 °C/1 h/w after cold-drawing.

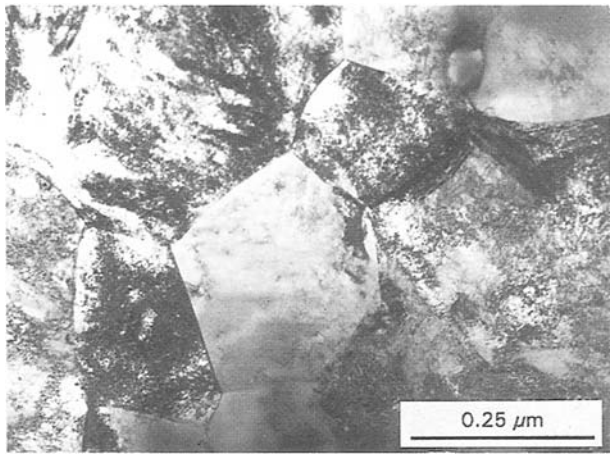

Figure 3 Structure of alloy annealed at 600 °C/1 h/w after cold-drawing.

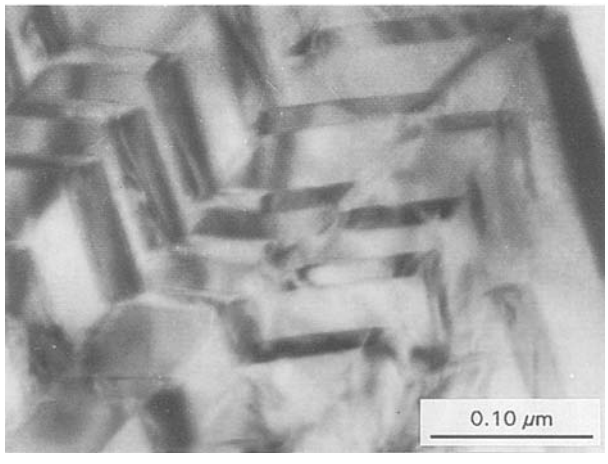

Figure 4 Structure of alloy annealed at 500 °C/1 h/w after cold-drawing, after predeformation to $\varepsilon_{rm} = 4.2\%$.

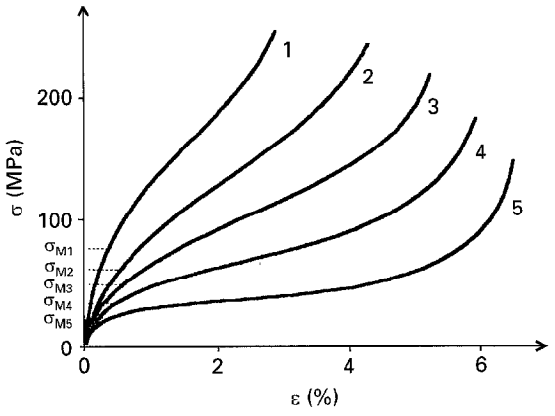

Figure 5 The stress–strain dependences of the investigated alloys: (1) work-hardened; annealed at (2) 400 °C; (3) 500 °C; (4) 600 °C and (5) 900 °C.

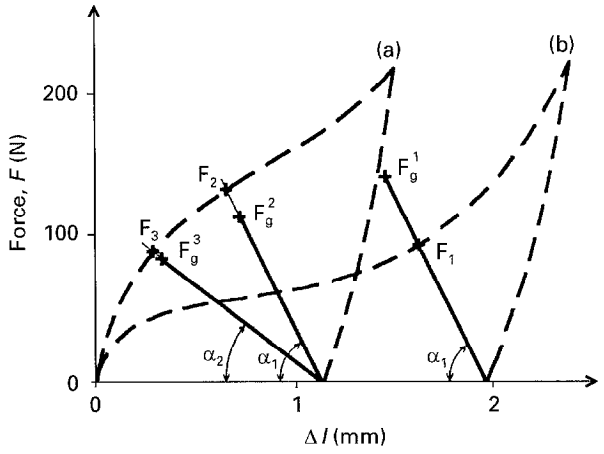

Figure 6 The working cycle of memory clamps with different structure. (a) 400 °C/1 h/water; (b) 900 °C/1 h/water.

with higher dislocation density. At the plateau, during the easy deformation, the transformation capacity is not exhausted in work-hardened materials and continues up to higher stresses. This is connected with apparently lower stiffness at higher stresses. If both B2 phase as well as martensite are present in the matrix, the deformation behaviour is analogous to the case of composite materials – the observed stiffness depends on both the properties of B2 and B19′ materials. Work hardening changes the transformation temperatures (lower M_s, higher A_f) and these changes also lead to an increase of critical stresses σ_{Mi}, necessary for SIM.

3.2.2. Recovery strains and generated forces

Both generated forces and reversible strains are strongly dependent on the opposite forces acting against the forces generated during the shape recovery process. Two extreme situations can be observed [23]:

- totally constrained conditions, where the recovery of the shape is not allowed by a rigid obstacle with very high stiffness; maximum force is generated at heating;
- free recovery without any opposite forces acting against the shape memory element; no forces are generated by the memory element during heating and shape recovery.

In the case of fixation clamps, the joined bones and surrounding tissues do not allow the predeformed shape memory clamp to shrink completely, but the clamp is not totally constrained and partial shape recovery occurs. The "working cycles" performed by two different TiNi shape memory clamps annealed at two different temperatures 400 and 900 °C, respectively, are schematically drawn in Fig. 6. The dotted curves characterize the force F versus elongation Δl dependences of the clamps during predeformation and unloading to the zero forces, and the solid lines represent the recovery of the shape and generation of compressive forces F_g on heating. The angles α_i between abscisa and solid lines represent the stiffness parameters $(SP)_i = dF/d\Delta l = \mathrm{tg}\,\alpha_i$ which correspond practically to the stiffness of the bones treated.

To have maximum recovery capacity, the maximum reversible strains at free recovery ε_{rm} were found for each material type. The specimens investigated were predeformed up to this strain level, when the forces generated were measured. The maximum ε_{rm} value of 6.25% was observed for clamps annealed at 900 °C. The clamps annealed at 600 °C possess the maximum reversible strain at free recovery of 4.3%, the specimens annealed at 500 °C, 4.2% and the specimens annealed at 400 °C 2.8% (every value is a mean of seven measurements). The maximum reversible strains of the work-hardened materials were measured by use of straight wires having corresponding lengths. The results obtained clearly demonstrate that the recovery strains are dependent on the dislocation density. The decrease of maximum recovery strain ε_{rm} is accompanied by increased work-hardening intensity leading to the modification of conditions at which the phase transformations occur. The higher the work-hardening stage the lower the B2/B19′ interface mobility and the martensite plates do not shrink accordingly and the result is a lower reversible strain [1, 4, 7].

As follows from Fig. 6 the forces F_g^i generated after heating to the same temperature depend on the stiffness parameter *SP*. For the higher stiffness, the generated force F_g^2 is higher than the force F_g^3 obtained for the lower value of the *SP*. The reversible deformation (shrinkage) of the clamps working against the higher stiffness is smaller compared with the reversible deformation obtained after heating the clamps in the system with the lower *SP*.

At the same stiffness parameter *SP* represented by the angle α_1, the highest force generated F_g^1 was detected in alloys annealed at 900 °C/1 h/water. The corresponding reversible deformation was highest in this case as well. In this material the dislocation density is low enough that the extent of reversible transformation controlled by the reversible movement of the B2/B19′ interfaces is considerable [1–4]. In contrast to this situation, reversible deformation at the same *SP* by the clamp annealed at 400 °C/1 h/water is the lowest. The reversible movement of B2/B19′ interfaces requires more energy because the moving interface interacts with obstacles (dislocations) and energy dissipation occurs. The opposite forces play a similar role

to the dislocations present in the matrix – they prevent reversible transformation. If the maximum opposite forces are lower, it means the stiffness parameter is lower (α_2 in Fig. 6), and the recoverable deformation is higher. This follows from the result that the forces generated can be effectively modified and the forces corresponding to the physiological conditions can be reached at an actual stiffness parameter SP by the use of optimal combined mechanical and heat treatment of the TiNi alloys. This is important, especially when the bone state is not optimal (e.g. osteoporosis). Based on the statistical data concerning the bone tissue stiffness and strength, an appropriate TiNi clamp can be used.

The character of the forces generated can alter after subsequent cooling down to body temperature. As evident from Fig. 6, the force F_g^1 generated after heating to a temperature above body temperature (as a rule to a temperature between 45 and 60 °C) decreases after subsequent cooling (to 37 °C) to the value F^1 in the case of clamps annealed at 900 °C/1 h/water. The greater the difference between the heating temperature and body temperature, the greater the decrease of force. This corresponds well with the results described in [15]. This decrease of the force generated by a clamp leads to the relaxation of the fixed system, with the bone fragments no longer being stabilized, and supporting immobilization is necessary. A different situation was observed in the clamps annealed at 400 °C/1 h/water where the generated forces F_g^2 and F_g^3 were lower than the forces F^2 and F^3 (Fig. 6), respectively. Analogous behaviour was observed in clamps annealed at 500 °C/1 h/water. It follows from the results obtained that by designing the fixation elements using memory alloys, the stiffness parameter and deformation behaviour of the memory material at body temperature have to be taken into account. These characteristics are at least as important as the transformation temperatures of the material used.

The clamps annealed at temperatures of 400 or 500 °C demonstrated a constant level of forces produced after heating and subsequent cooling to 37 °C. This is a consequence of the above-mentioned work-hardening effect, which significantly changes the conditions for martensite formation [1, 4, 8, 9] and the individual stress–strain dependence (see Figs 5 and 6).

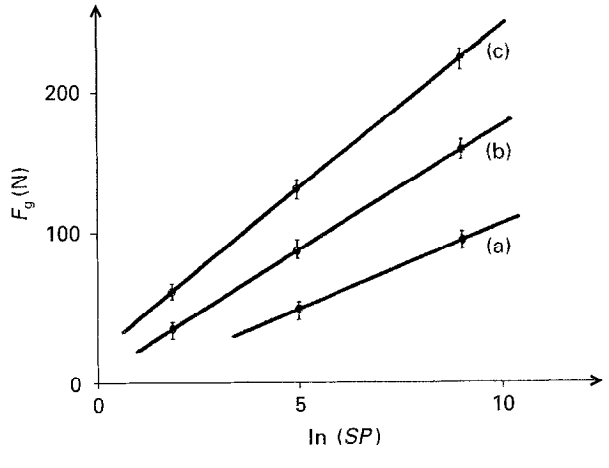

Figure 7 Relationship between the generated forces F_g and the stiffness parameter (SP) after heating to temperature (a) 45 °C; (b) 50 °C; (c) 80 °C.

In contrast to alloys with lower dislocation density and coarser grains (alloys annealed at 600 and 900 °C), the fine-grained alloys with higher dislocation density (those annealed at 400 and 500 °C) have higher σ_{Mi} stresses.

The difference ΔF between the force F_g^i generated after heating to a temperature between 45 and 80 °C and the force F^i necessary for SIM formation at 37 °C corresponds to the decrease of compressive fixation forces and to the instability of clamps annealed at 600 and 900 °C.

It follows from the results obtained that the relationship between the generated force F_g and the stiffness parameter SP can be characterized, for a constant heating temperature, by the logarithmic equation:

$$F_g = A + B \ln(SP)$$

where A and B are calculated constants. The forces generated increase with increased clamp temperature, as evident from Fig. 7, because the opposing external forces (dependent on SP) stabilize the B19′ martensite (increase of A_s, A_f temperatures) [1, 4].

4. Discussion of medical applications

Having a material with optimized structural features (tested both under laboratory conditions and

Figure 8 An example of a corrective osteotomy of the first metatarsus. Acceptable compression of the fragments involved is achieved after TiNi clamps have been warmed up (black arrow). Using two clamps a more stable osteofixation is assured.

experimentally with animals available), therapeutic applications have been in progress since 1993. In a total of 68 patients, the clamps in small bone fracture treatments and artificial osteotomies treatments have been put to use. Till now we have applied our TiNi clamps for the following purposes: hallux valgus correction (Fig. 8), metatarsa-cuneiforme arthrodesis, desis of the first carpometacarpal joint and interphalangeal joint, fixation of a pseudoarthrosis of the metatarsal bone, correction of malunion of the finger (Fig. 9). A special area of interest lies in delayed union and non-union of the carpal scaphoid (Fig. 10).

In contradistinction to "classic" metal staples (generally made from titanium alloys) which guarantee the passive stability of bone fragments, the TiNi memory clamps compress the fragments. The compressive forces are produced as a consequence of the shape memory effect and have to be optimized with respect to physiological needs. The optimal physiological forces are dependent on four main factors: the stiffness and remodellation rate of the bone; the temperature which is reached during heating of the shape memory clamp; the dimensions and shape of the TiNi clamp; and the structure of the TiNi alloy. It is well known that both the extent of recovery stresses as well as recovery strains occurring during the shape memory effect depend on the structural state of the TiNi alloy [6–9] and on the stiffness of the bone. The aim of the latest trend is to have at our disposal the smallest possible implant allowing the smallest invasion. In contrast to shape memory alloy elements developed previously [15, 18, 19], our TiNi memory clamps do not need to be cooled before predeformation and can be further adjusted at room temperature if required. A very important characteristic is that the forces generated after heating the memory clamps do not decrease after cooling to body temperature. Clamps with an optimized structure are supplied in a predeformed state and after X-ray sterilization can be inserted in a human body. If necessary, the clamps can be remodelled by the surgeon at room temperature before implantation. The force generated after heating the implant enables compressive osteosynthesis.

The reduction or even exclusion of the immobilization period, which facilitates a rehabilitation programme, is very important. Using our TiNi clamps, we did not apply cast splints longer than it took for the soft tissue condition to be under control. The immobilization period never exceeded 12 days. In the case of the Shapiro internal fixation systems, a cast immobilization of 4 to 6 weeks has usually been recommended [24–26]. We believe, the short duration of immobilization represents, beside stable fixation, the most important advantage of this recently developed system.

Figure 9 A further possible application: a treatment of a malunion of an index finger by corrective rotatory osteotomy. Using the TiNi clamp, stable fixation was gained.

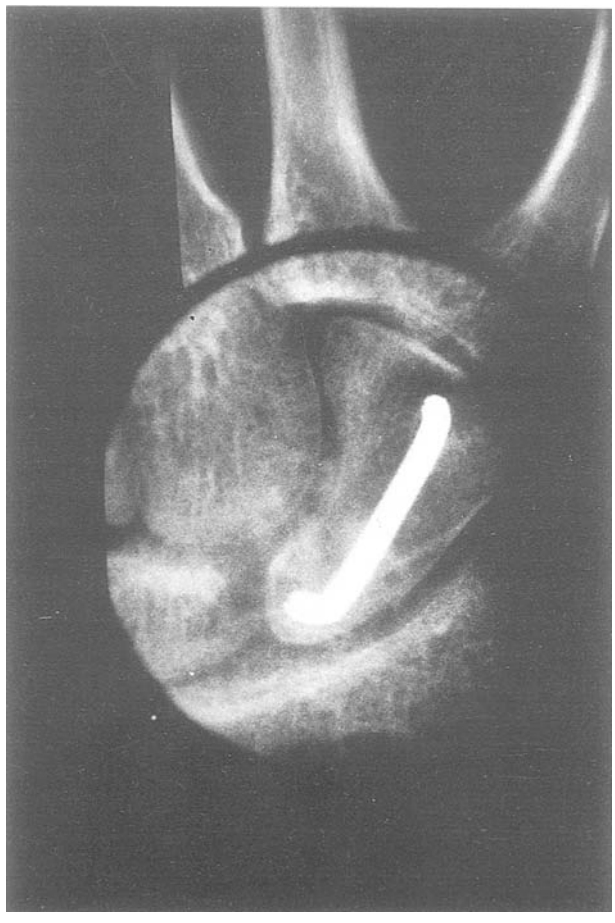

Figure 10 Another demonstration of the usability of a TiNi clamps for fixation in the treatment of pseudoarthrosis of the carpal scaphoid. Obtaining stability in this particular case does not require any supporting fixation, thus enabling active rehabilitation to start immediately following surgery.

5. Conclusions

Modifying the conditions at which the martensitic and reverse transformation in TiNi alloys occur (the combination of work hardening and an appropriate annealing procedure) can lead to the optimal structure and properties of shape memory TiNi clamps.

As a consequence of different treatment procedures, transformation temperature changes were observed. The "yield point" σ_{Mi}, the "elastic moduli" of shape memory TiNi alloys, the extent of reversible strains and the mobility of B2/B19′ interfaces are influenced by the work-hardening intensity. The level of forces generated F_g depends on the stiffness parameter of the system and the temperature reached. From the point of view of the stability of the force generated after heating and subsequent cooling to human body temperature, annealing at 400 or 500 °C following a 15% cold-working reduction is optimal.

The stability of the bone fragments involved enables us to start an active rehabilitation programme very soon after surgery, when wound healing begins to come under control, generally after two or three days in our patients. We believe that this optimal compressive stabilization facilitates recovery, as a general principle. Both further clinical testing and histological assessment are required.

Acknowledgements

The authors are pleased to acknowledge the financial support of this research by the Grant Agency (GACR) of the Czech Republic under grant 106/93/0736. The authors are grateful to Dr V. Kafka (UTAM Academy of Science of Czech Republic AVCR Prague) for providing the results of TiNi alloys biocompatibility tests.

References

1. H. WARLIMONT, L. DELAEY, R. V. KRISHNAN and H. TAS, *J. Mater. Sci.* **9** (1974) 1545.
2. L. DELAEY and J. THIENEL, in "Shape memory effect in alloys", edited by J. Perkins (Plenum Press, New York, 1975) p. 197.
3. K. OTSUKA and K. SHIMIZU, *Int. Met. Rev.* **31** (1986) 93.
4. P. FILIP, PhD theses, TU Ostrava (1988) (in Czech).
5. P. FILIP and K. MAZANEC, *Scripta Met. Mater.* **30** (1994) 67.
6. P. FILIP, J. RUSEK and K. MAZANEC, *Z. Metallkunde* **82** (1991) 488.
7. P. FILIP and K. MAZANEC, *Mater. Sci. Eng.* **A159** (1992) L5.
8. P. FILIP, V. MATYSEK and K. MAZANEC, *Z. Metallkunde* **83** (1992) 877.
9. P. FILIP and K. MAZANEC, *Mater. Sci. Eng.* **A147** (1994) L41.
10. P. FILIP, J. PECH and K. MAZANEC, *Berg- und Hüttenmännische Monatshefte* **139** (1994) 174.
11. CH. YIUYING, CH. JINFANG, L. RUNDONG, Y. LIPING and Z. MING, in "Shape memory materials '94", edited by Y. Chu and H. Tu (International Academic Publishers, Beijing, 1994) p. 181.
12. L. S. CASTLEMAN, V. L. MOTZKIN, F. P. ALICANDRI, V. C. BONAWIT and A. A. JOHNSON, *J. Biomed. Mater. Res.* **10** (1976) 695.
13. L. S. CASTLEMAN and S. M. MOTZKIN, in "Biocompatibility of clinical implant materials", edited by D. F. Williams (CRC, Boca Raton, FL, 1981) p. 129.
14. Y. OSHIDA, R. SACHDEVA, S. MIYAZAKI and S. FUKUYO, *Mater. Sci. Forum* **56–58** (1990) 705.
15. G. BENSMANN, F. BAUMGART and J. HAASTERS, *Technische Mitteilungen Krupp Forschungs-Berichte* **40** (1982) 123.
16. D. STÖCKEL, "Legierungen mit Formgedächtnis" (Kontakt & Studium, Expert Verlag, München, 1988).
17. C. M. WAYMAN, *J. Metals* **32** (1980) 129.
18. Y. N. ZHUK, "Advanced medical applications of shape memory alloy in Russia" (TETRA Consult, Moscow State University, Moscow, 1994).
19. V. E. GJUNTER, L. A. MONASEVICH, J. I. PASKAL and D. B. TSCHERNOV, in "Effekty pamjati formy i ikh primenenie v medicine", edited by L. A. Monasevich *et al.* (Nauka, Novosibirsk, 1992).
20. P. FILIP and K. MAZANEC, *Mater. Sci. Eng.* **A127** (1990) L19.
21. M. PIAO, K. OTSUKA, S. MIYAZAKI and H. HORIKAWA, *Mater. Trans. JIM* **34** (1993) 919.
22. J. ORTIN and A. PLANNES, *Acta Metall.* **36** (1988) 1873.
23. T. W. DUERING, *Mater. Sci. Forum* **56–58** (1990) 679.
24. S. SHAPIRO, *J. Hand Surg.* **12A** (1987) 218.
25. O. L. KORKALA, O. M. KUOKANNEN and M. S. EEROLA, *J. Bone Joint Surg.* **74A** (1992) 423.
26. W. SIEKMANN, in "Surgical techniques for the Shapiro internal fixation system in hand surgery" (3 M Co., Basel, 1991).

Received 30 June
and accepted 20 November 1995